International Journal of Bifurcation and Chaos, Vol. 12, No. 1 (2002) 115–128

ON THE SPATIAL ENTROPY AND PATTERNS OF TWO-DIMENSIONAL CELLULAR NEURAL NETWORKS

SONG-SUN LIN*
Department of Applied Mathematics, National Chiao-Tung University, Hsin-Chu 30050, Taiwan

TZI-SHENG YANG
Department of Applied Mathematics, I-Shou University, Kaohsiung 84041, Taiwan

Received April 20, 2000; Revised March 9, 2001

This work investigates binary pattern formations of two-dimensional standard cellular neural networks (CNN) as well as the complexity of the binary patterns. The complexity is measured by the exponential growth rate in which the patterns grow as the size of the lattice increases, i.e. spatial entropy. We propose an algorithm to generate the patterns in the finite lattice for general two-dimensional CNN. For the simplest two-dimensional template, the parameter space is split up into finitely many regions which give rise to different binary patterns. Qualitatively, the global patterns are classified for each region. Quantitatively, the upper bound of the spatial entropy is estimated by computing the number of patterns in the finite lattice, and the lower bound is given by observing a maximal set of patterns of a suitable size which can be adjacent to each other.

1. Introduction

The cellular neural network (CNN), as designed by Chua and Yang [1988a, 1988b], is an array of an identical system of cells that are locally coupled. This work investigates the complexity of stable binary patterns of two-dimensional CNN. Indeed, the state equation of a cell C_{ij} is the set of coupled O.D.E's

$$\dot{x}_{ij}(t) = -x_{ij}(t) + \sum_{|k|,|l|\le d} a_{kl} y_{i+k,j+l}(t) + z, \quad i,j \in \mathbb{Z}^2, \tag{1}$$

with output $y_{ij}(t) = f(x_{ij}(t))$. Here $f(\cdot)$ is a piecewise-linear function expressed as

$$f(x) = \frac{1}{2}(|x+1| - |x-1|)\,. \tag{2}$$

The parameter z is a time-invariant bias and d is a positive integer. The coupling parameters a_{kl}'s are assumed to be space-invariant, which is arranged in a $(2d+1)\times(2d+1)$ matrix A called a *template*.

The stationary solutions $\mathbf{x} = (x_{ij})$ of (1) are prerequisite for understanding the CNN dynamics. Indeed, when studying the long-time behavior of a dynamic system, the stationary solutions are the simplest objects to be considered. In the case of CNN with finite cells and symmetric template A, Chua and Yang [1988a], Lin and Shih [1999] demonstrated that every trajectory of (1) tends to an equilibrium as time proceeds. The stationary solutions $\mathbf{x} = (x_{ij})$ of (1) satisfy

$$x_{ij} = z + \sum_{|k|,|l|\le d} a_{kl} f(x_{i+k,j+l}), \quad i,j \in \mathbb{Z}\,. \tag{3}$$

*This research was partially supported by the National Science Council of the Republic of China under Contract No. NSC 88-2115-M-259-003.

A stationary $\mathbf{x}$ solution is called a mosaic solution if $|x_{ij}| > 1$ for all $i, j \in \mathbb{Z}$. The corresponding output $\mathbf{y} = (f(x_{ij}))$ is called a mosaic pattern. The mosaic solution of (1) is always locally asymptotically stable [Juang & Lin, 1997] (and the references given therein). Among all stationary solutions, the stable mosaic solutions, which have been studied before [Juang & Lin, 1997], are the most fundamental and important applications (finite cells) in image-processing [Chua, 1988b, 1988]. Those investigations addressed two problems directly related to the mosaic patterns: (a) the directed problem, in which the parameter space is partitioned into finitely many regions so that in each region (1) has the same patterns and (b) the complexity of global patterns.

The complexity of mosaic solutions can be examined according to its entropy. For completeness, the following discussion introduces some definitions and results concerning spatial entropy. Further details can be found in [Chow *et al.*, 1996a]. Denote by $\{-1, 1\}^{\mathbb{Z}^2}$ the set of all $\mathbf{y} : \mathbb{Z}^2 \to \{-1, 1\}$ i.e. the set of all mosaic patterns. Let $\mathcal{U}$ be a translation-invariant subset of $\{-1, 1\}^{\mathbb{Z}^2}$ and $\mathbb{Z}_{mn} = \{(i, j) : 1 \le i \le m, 1 \le j \le n\}$. The number of distinct patterns observed among the elements of $\mathcal{U}$ when observation is restricted to subset $\mathbb{Z}_{mn}$, is denoted by $\Gamma_{mn}(\mathcal{U})$. The spatial entropy $h(\mathcal{U})$ of $\mathcal{U}$ is defined by

$$h(\mathcal{U}) = \lim_{m,n\to\infty} \frac{\ln \Gamma_{mn}(\mathcal{U})}{mn}\,.$$

$\mathcal{U}$ is called *spatial chaos* if the spatial entropy $h(\mathcal{U})$ is positive. Otherwise, $\mathcal{U}$ is called *pattern formation*.

The case of a two-dimensional template markedly differs from that of a one-dimensional template. In the case of the one-dimensional template, the transition matrix can be used to construct the global pattern; the exact spatial entropy is then computed [Lin & Yang, 2000]. However, the transition matrix cannot be defined in the case of a two-dimensional template. Up to now, no efficient and general method is available for two-dimensional templates. In [Juang & Lin, 1997] and [Shih, 1998], are discussed two-dimensional symmetric and asymmetric square cross templates, respectively. The direct problem is completely solved in both cases and the global patterns are classified by building blocks and the corresponding compatible conditions. In addition, the spatial chaos is confirmed to occur by identifying the blocks which can be adjacent to each other. In contrast to the above developments, this work presents a novel algorithm to generate the patterns in the finite lattice for a general template, which gives the upper bound of the spatial entropy. Moreover, the lower bound of the spatial entropy is estimated by obtaining the maximal set of the patching blocks of some size (depending on the characteristic of global patterns). This investigation concentrates mainly on the simplest two-dimensional template, L-shaped liked, i.e.

$$A = \begin{pmatrix} 0 & r & 0 \\ 0 & p & s \\ 0 & 0 & 0 \end{pmatrix}.$$

The tools developed herein can be easily applied to the general templates. For example, the case of a fully connected template

$$A' = \begin{pmatrix} a_1 & a_2 & a_3 \\ a_4 & a_5 & a_6 \\ a_7 & a_8 & a_9 \end{pmatrix},$$

the reader can go through the process of partitioning parameter space, determining the feasible local patterns as in Sec. 2, then finding the patterns in a finite lattice by using an algorithm similar to the one in Sec. 3. All the process are very similar to the case of template A except the shape of the local patterns.

Generally, a neural network concerns the relationship between input and output patterns. A learning algorithm is used to establish this relationship. Such a learning algorithm usually starts with initial weights i.e. coupling parameters of the neural network and then consecutively updates the weights according to the difference between actual output and desired output patterns. Our investigation provides a method (for CNN) to analyze (a) possible output patterns in different regions of parameter space, (b) the choice of the range of coupling parameters in the learning process.

The rest of this paper is organized as follows. Section 2 addresses the direct problem. The method is quite similar to the case of the one-dimensional template [r p s][Lin & Yang, 2000]. Section 3 presents a novel algorithm to generate the patterns in the finite lattice and give the upper bound of the spatial entropy. Section 4 describes and classifies the global patterns. For the case of spatial chaos, we find the maximal set of patching blocks of some

size (depending on the characteristic of global patterns) and give the lower bound of the spatial entropy. Conclusions are finally made in Sec. 5.

2. Partitioning the Parameter Space

First, we introduce the notation of local patterns [Juang & Lin, 1997; Hsu *et al.*, 2000] for the template

$$A = \begin{pmatrix} 0 & r & 0 \\ 0 & p & s \\ 0 & 0 & 0 \end{pmatrix}.$$

The state equation (1) now becomes

$$\dot{x}_{ij}(t) = r y_{i-1,j}(t) + s y_{i,j+1}(t) + p y_{ij}(t) + z - 1\,. \tag{4}$$

For a mosaic solution $\mathbf{x}$, the output at cell C_{ij} is $+1$, i.e. $x_{ij} > 1$ if and only if

$$r y_{i-1,j} + s y_{i,j+1} + p + z - 1 > 0\,, \tag{5}$$

and, similarly, the output at cell C_{ij} is -1, i.e. $x_{ij} < -1$ if and only if

$$r y_{i-1,j} + s y_{i,j+1} - p + z + 1 < 0\,. \tag{6}$$

Denote by $\mathbf{X}^2 = \{-1, 1\}^2$ the set of all possible $(y_{i-1,j}, y_{i,j+1})$. Each $(k, m) \in \mathbf{X}^2$ is naturally associated with two local patterns $P_{k,m}$ and $N_{k,m}$, which have y_{ij} "+1" and y_{ij} "−1", respectively. Visually, the "+1" and "−1" are represented by black and white squares, respectively.

$$P_{1,1} = \begin{smallmatrix}\blacksquare\blacksquare\\ \blacksquare\blacksquare\end{smallmatrix}\,, \quad N_{1,1} = \begin{smallmatrix}\blacksquare\blacksquare\\ \square\blacksquare\end{smallmatrix}\,,$$

$$P_{1,-1} = \begin{smallmatrix}\blacksquare\blacksquare\\ \blacksquare\square\end{smallmatrix}\,, \quad N_{1,-1} = \begin{smallmatrix}\blacksquare\blacksquare\\ \square\square\end{smallmatrix}\,,$$

$$P_{-1,1} = \begin{smallmatrix}\square\blacksquare\\ \blacksquare\blacksquare\end{smallmatrix}\,, \quad N_{-1,1} = \begin{smallmatrix}\square\blacksquare\\ \square\blacksquare\end{smallmatrix}\,,$$

$$P_{-1,-1} = \begin{smallmatrix}\square\blacksquare\\ \blacksquare\square\end{smallmatrix}\,, \quad N_{-1,-1} = \begin{smallmatrix}\square\blacksquare\\ \square\square\end{smallmatrix}\,.$$

Obviously, for a given template A and threshold z, $P_{k,m}$ and $N_{k,m}$ are feasible if and only if (7) and (8) hold, respectively.

$$z + (p-1) + kr + ms > 0\,, \tag{7}$$

$$z - (p-1) + kr + ms < 0\,. \tag{8}$$

The set of feasible local patterns, denoted by $\mathcal{F}(A, z)$, is defined to be the collection of feasible $P_{k,m}$'s and $N_{k,m}$'s.

The parameter space, $\mathcal{P}^4 = \{(r, s, p, z) | z, p, r, s \in \mathbb{R}\}$, can be partitioned according to the feasible local patterns. To partition the r-s plane, we first arrange the elements of $\mathbf{X}^2$ according to the value of $kr + ms$. Denote by $I[i, j]$ the set of integers are not smaller than i and not larger than j. Given a (r, s), the (r, s)-*arrangement* of $\mathbf{X}^2$ is a function from $\mathbf{X}^2$ into $I[1, 4]$, which assigns the integer i to (k_0, m_0) provided that $k_0 r + m_0 s$ is the ith largest among all of $kr + ms$, $(k, m) \in \mathbf{X}^2$. It can be verified that the following half lines, $L_1, \ldots, L_8$, denoted by

$$L_1 : r > 0,\ s = 0\,, \quad L_2 : r > 0,\ r = s\,,$$
$$L_3 : r = 0,\ s > 0\,, \quad L_4 : r > 0,\ r = -s\,,$$
$$L_5 : r < 0,\ s = 0\,, \quad L_6 : r < 0,\ r = s\,,$$
$$L_7 : r = 0,\ s < 0\,, \quad L_8 : r > 0,\ r = -s\,,$$

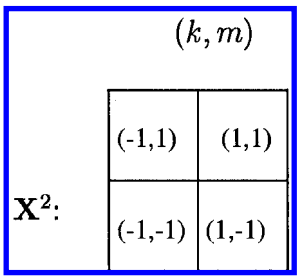

Fig. 1.

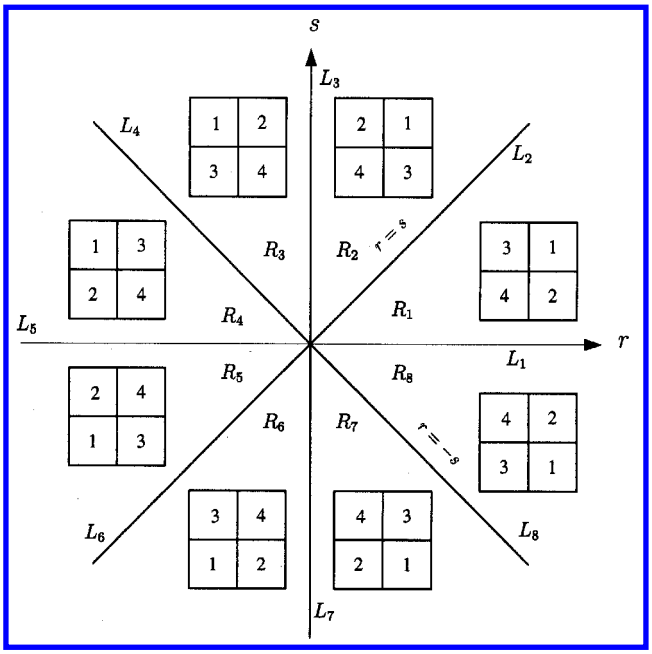

Fig. 2. Partition of r–s plane according to (r, s)-arrangement.

divide the $r - s$ plane into eight open regions, $R_1, \ldots, R_8$. Here R_i is the open region bounded by L_i and L_{i+1}, for $1 \le i \le 7$ and R_8 is the open region bounded by L_8 and L_1 such that only one (r, s)-arrangement of $\mathbf{X}^2$ is induced in each R_i (see Fig. 2). Denote by J_i, the (r, s)-arrangement of $\mathbf{X}^2$ induced in R_i.

Figure 2 is illustrated as follows: Each element (k, m) of $\mathbf{X}^2$ corresponds to a position in a 2×2 lattice as shown in Fig. 1. On each R_i, there is also a 2×2 lattice and the values of $J_i(k, m)$ are put into the position of this lattice, which corresponds to (k, m).

Now, we partition $z-p$ plane when (r, s) in R_i. If $J_i(k, m) = j$, let ℓ_j^+ and ℓ_j^- be the lines on $z - p$ plane with equations:

$$z + (p - 1) + kr + ms = 0\,, \tag{9}$$

and

$$z - (p - 1) + kr + ms = 0\,, \tag{10}$$

respectively. Therefore $\{\ell_j^+\}_{j=1}^4$ and $\{\ell_j^-\}_{j=1}^4$ form two sets of parallel lines in the $z - p$ plane with ℓ_{j+1}^+ and ℓ_j^- lying above ℓ_j^+ and ℓ_{j+1}^-, respectively. Let $[\mu, \nu]_i$, $0 \le \mu, \nu \le 4$, denote the open region bounded by $\ell_\mu^+, \ell_{\mu+1}^+, \ell_{5-\nu}^-, \ell_{4-\nu}^-$ with $\ell_0^+, \ell_0^-, \ell_5^+, \ell_5^-$ being the empty lines, as observed in Fig. 3. Hence, the $z-p$ plane is partitioned into finitely many disjoint regions, i.e. $[\mu, \nu]_i$, $0 \le \mu, \nu \le 4$. After partitioning the parameter space, Theorem 2.1 indicates how the feasible local patterns are determined for each region $[\mu, \nu]_i$.

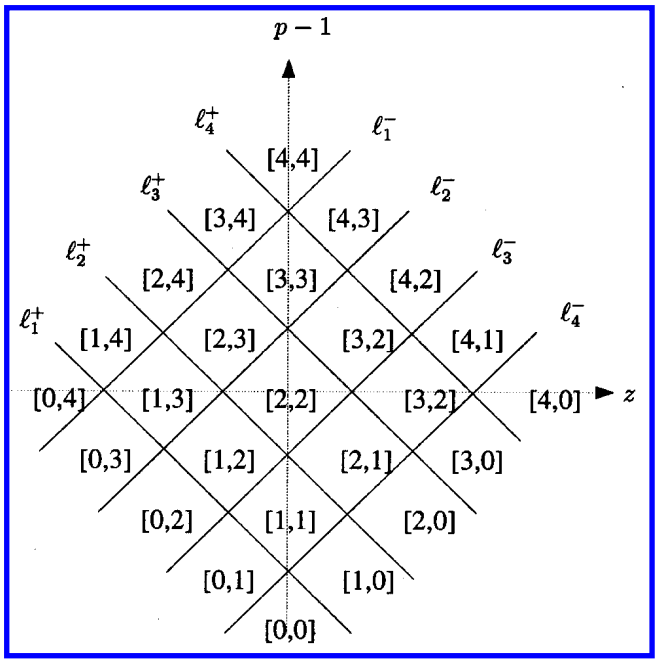

Fig. 3.

Theorem 2.1. *For $(z, p) \in [\mu, \nu]_i$, the feasible local patterns are exactly the union of*

$$\bigcup_{J_i(k,m) \le \mu} P_{k,m}$$

and

$$\bigcup_{J_i(k,m) \ge 5-\nu} N_{k,m}\,.$$

Proof. Assume $J_i(k_1, m_1) = \mu$, $J_i(k_2, m_2) = \mu + 1$ and $(z, p) \in [\mu, \nu]_i$. According to the definition of $[\mu, \nu]_i$, z and p satisfy

$$z + (p - 1) + k_1 r + m_1 s > 0\,, \tag{11}$$

and

$$z + (p - 1) + k_2 r + m_2 s < 0\,, \tag{12}$$

which implies that

$$\begin{aligned} &z + (p - 1) + kr + ms > 0 \\ \text{if}\quad &J_i(k, m) \le J_i(k_1, m_1) = \mu\,, \end{aligned} \tag{13}$$

and

$$\begin{aligned} &z + (p - 1) + kr + ms < 0 \\ \text{if}\quad &J_i(k, m) \ge J_i(k_2, m_2) = \mu + 1\,. \end{aligned} \tag{14}$$

In addition, there is no (k, m) such that $\mu < J_i(k, m) < \mu + 1$. Hence, $\bigcup_{J_i(k,m) \le \mu} P_{k,m}$ are exactly the feasible local patterns whose left-lower cell is $+1$. A similar argument shows that $\bigcup_{J_i(k,m) \ge 5-\nu} N_{k,m}$ are exactly the feasible local patterns whose left-lower cell is -1. The proof is complete. ■

Example 2.1. If $r = 2$, $p = 3/2$, $s = 1$ and $z = 0$, a mosaic solution (x_{ij}) satisfies

$$x_{ij} = \frac{3}{2} y_{ij} + 2y_{i-1,j} + y_{i,j+1},\ (i, j) \in \mathbb{Z}^2\,.$$

To consider which local patterns are feasible, (a) $y_{ij} = 1$ implies $x_{ij} = 3/2 + 2y_{i-1,j} + y_{i,j+1} > 1$, hence

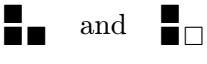 and

are feasible. (b) $y_{ij} = -1$, implies $x_{ij} = 3/2 + 2y_{i-1,j} + y_{i,j+1} < -1$, hence

$$\begin{smallmatrix}\square & \\ \square & \square\end{smallmatrix} \quad \text{and} \quad \begin{smallmatrix}\square & \\ \square & \blacksquare\end{smallmatrix}$$

are feasible.

On the other hand, we can also induce the feasible local patterns by Theorem 2.1 as follows. $(r, s) = (2, 1) \in R_1$ implies

$$\ell_1^+ : z + (p-1) + 3 = 0, \ \begin{smallmatrix}\blacksquare & \\ \blacksquare & \blacksquare\end{smallmatrix}; \quad \ell_1^- : z - (p-1) + 3 = 0, \ \begin{smallmatrix}\square & \\ \square & \square\end{smallmatrix};$$

$$\ell_2^+ : z + (p-1) + 1 = 0, \ \begin{smallmatrix}\blacksquare & \\ \blacksquare & \square\end{smallmatrix}; \quad \ell_2^- : z - (p-1) + 1 = 0, \ \begin{smallmatrix}\square & \\ \square & \blacksquare\end{smallmatrix};$$

$$\ell_3^+ : z + (p-1) - 1 = 0, \ \begin{smallmatrix}\square & \\ \blacksquare & \blacksquare\end{smallmatrix}; \quad \ell_3^- : z - (p-1) - 1 = 0, \ \begin{smallmatrix}\blacksquare & \\ \square & \square\end{smallmatrix};$$

$$\ell_4^+ : z + (p-1) - 3 = 0, \ \begin{smallmatrix}\square & \\ \blacksquare & \square\end{smallmatrix}; \quad \ell_4^- : z - (p-1) - 3 = 0, \ \begin{smallmatrix}\blacksquare & \\ \square & \blacksquare\end{smallmatrix}.$$

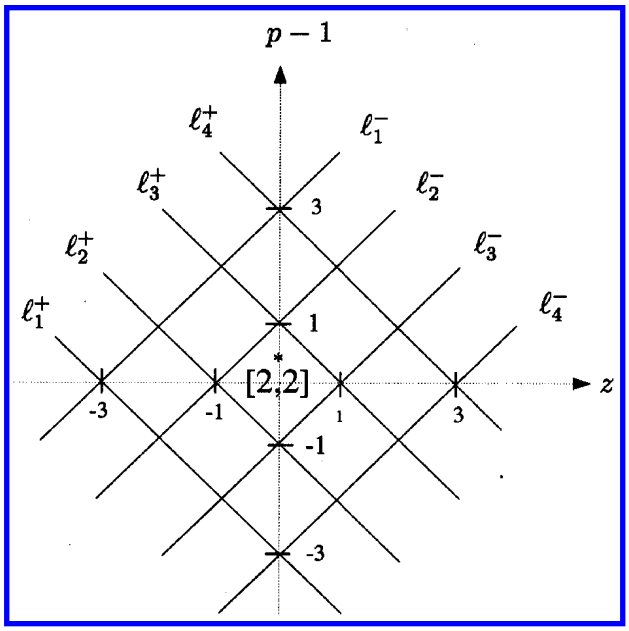

Fig. 4. Partition of $z - p$ plane when $(r, s) = (2, 1)$.

Figure 4 shows that $(z, p) \in [2, 2]$, according to Theorem 2.1, which implies the local patterns associated with ℓ_1^+, ℓ_2^+, ℓ_3^- and ℓ_4^- are feasible i.e.

$$\begin{smallmatrix}\blacksquare & \\ \blacksquare & \blacksquare\end{smallmatrix}, \quad \begin{smallmatrix}\blacksquare & \\ \blacksquare & \square\end{smallmatrix}, \quad \begin{smallmatrix}\blacksquare & \\ \square & \square\end{smallmatrix}, \quad \begin{smallmatrix}\blacksquare & \\ \square & \blacksquare\end{smallmatrix}.$$

3. An Algorithm to Generate the Patterns in the Finite Lattice

Herein, the patterns in the finite lattice can be constructed based on the feasible local patterns. Indeed, assume that we have the set of feasible local patterns $\mathcal{F}(A, z) = \{U_1, \ldots, U_k\}$ where U_i has the shape $\begin{smallmatrix}\square & \\ \square & \square\end{smallmatrix}$. We dilate U_i to the minimal rectangular block containing U_i by adding a black or white block in the upper right corner. By doing so, we obtain the set of patterns of 2×2 size corresponding to $\mathcal{F}(A, z)$, say $\mathcal{G} = \{V_1, \ldots, V_{2k}\}$. Starting from $\mathcal{G}$, we use the technique of [Lin & Yang, 2000] by gluing right or below to obtain the patterns of larger size [Lin & Yang, 2000]. The patterns in finite lattice can be obtained by executing the following algorithm.

Algorithm

Initially set $\mathcal{G} = \{V_1, \ldots, V_{2k}\}$. Repeat executing (A) and (B) in suitable order. The patterns in the lattice of any finite size can be attained.

(A) One step horizontal extension.

(i) Suppose that each pattern in $\mathcal{G}$ is of size $m \times n$. From $\mathcal{G}$, take all pairs (V_i, V_j) such that V_i can glue to V_j on the right with overlapping $m - 1$ columns, i.e. the last $m - 1$ columns of V_i must equal to the first $m-1$ columns of V_j, respectively. Such a pair is referred to herein as a *horizontal compatible pair of patterns*.

(ii) Refresh $\mathcal{G}$ as the set of patterns obtained by gluing the horizontal compatible pairs of patterns in (i) together with overlapping $m - 1$ columns. Then, $\mathcal{G}$ is now the set of patterns of size $m \times (n + 1)$.

(B) One step vertical extension.

(i) Suppose that each pattern in $\mathcal{G}$ is of size $m \times n$. From $\mathcal{G}$, take all pairs (V_i, V_j)

such that V_i can glue to V_j below with overlapping $m-1$ rows, i.e. the last $m-1$ rows of V_i are equal to the first $m-1$ rows of V_j, respectively. Such a pair are referred to herein as a *vertical compatible pair of patterns*.

(ii) Refresh $\mathcal{G}$ as the set of the patterns obtained by gluing the vertical compatible pairs of patterns in (i) together with overlapping $m-1$ rows. Then, $\mathcal{G}$ is now the set of patterns of size $(m+1)\times n$.

For fixed A and z, let $\overline{h}_{m,n} = (\ln \Gamma(m,n))/(mn)$, which can be obtained by executing (A) m times and (B) n times. Proposition 3.1 shows the properties of $\overline{h}_{m,n}$.

Proposition 3.1. *$\{\overline{h}_{2^k m,2^k n}\}_{k=1}^{\infty}$ is a decreasing sequence and converge to the spatial entropy of mosaic patterns.*

Proof. First, we claim that $\overline{h}_{2m,2n} \le \overline{h}_{m,n}$. In a $2m \times 2n$ lattice, there are 2×2 disjoint blocks of size $m \times n$. When constructing the patterns in the lattice, each block has at most $\Gamma(m, n)$ choices i.e. $\Gamma(2m, 2m) \le (\Gamma(m, n))^{2\times 2}$. Hence $\overline{h}_{2m,\,2n} \le \overline{h}_{m,n}$ follows immediately. The standard induction argument shows that $\{\overline{h}_{2^k m,2^k n}\}_k$ is decreasing and its limit follows from the definition of the spatial entropy of the mosaic patterns. The proof is complete. ■

Proposition 3.1 suggests the upper bound of the spatial entropy $\overline{h}_{m,n}$. However, the computation of $\Gamma(m, n)$ consumes considerable amounts of time and memory as the spatial chaos occurs. Therefore we need a procedure to confirm the spatial chaos for some regions.

4. Global Patterns and Spatial Chaos

In this section, we construct the global patterns for each region $[\mu, \nu]_i$ of the parameter space. According to the feasible local patterns for each region, we induce and describe the class of global patterns. However, once spatial chaos occurs, the number of restrictions of the global patterns in the finite lattice grows too fast to compute even though the class of the global patterns can be characterized. To confirm spatial chaos, we give the maximal set of the *patching blocks* of some size (depending on the characteristic of the global patterns). Restated, the set contains the largest number of blocks of some size, which can be adjacent to each other. Through this process, we give the lower bound of the spatial entropy.

First, we introduce some special subsets of $\mathbb{Z}^2$, which are necessary to describe global patterns.

Definition 4.1. [Juang & Lin, 1997] A horizontal (resp. vertical) edge of length k in $\mathbb{Z}^2$ is the subset defined U by $U = \{(i, j_0) : i \in [i_1, i_2]\}$ for some $i_1, i_2 \in \mathbb{Z}$ ($U = \{(i_0, j) : j \in [j_1, j_2]\}$ for some $j_1, j_2 \in \mathbb{Z}$ respectively). A edge of infinite length is called a line. The solid edge $\tilde{U}$ of U in $\mathbb{R}^2$ is defined by $\tilde{U} = \{(x, j_0) : i_1 \le x \le i_2\}$ (vertical case is similarly defined). A union of edges T in $\mathbb{Z}^2$ is called a path if (i) T contains no 2×2 lattice (i.e. width one) and (ii) the solid path $\tilde{T}$ of T, i.e. the union of the corresponding solid edges, is connected. A path T in $\mathbb{Z}^2$ is nonincreasing (resp. nondecreasing) if (i, j) belongs to T implies $(i+1, j+1)$ (resp. $(i+1, j-1)$) does not belong to T.

Comment. A horizontal or vertical edge is both nonincreasing and nondecreasing paths according to Definition 4.1.

Since the patterns for $[\mu, \nu]_i$ and $[\nu, \mu]_i$ have opposite colors, it is sufficient to discuss only the cases of $[\nu, \mu]_i$ with $\mu \ge \nu$ and $1 \le i \le 4$. Herein, we first state the result of this section.

Theorem 4.1. *Equation (4) is spatial chaos if and only if r, s, p and z belong to the following regions of $\mathcal{P}^4$:*

1. $[4, 4]_i$, $1 \le i \le 8$.
2. $[4, 3]_i$, $1 \le i \le 8$.
3. $[4, 2]_i$, $i = 4, 5, 6, 7$.
4. $[4, 1]_i$, $i = 5, 6$.
5. $[3, 3]_i$, $1 \le i \le 8$.
6. $[3, 2]_i$, $i = 4, 5, 6, 7$.

Furthermore, we observe that $[\mu, \nu]_i$ with $\min(\mu, \nu) \ge 3$ is always spatial chaos for each i.

The proof of Theorem 4.1 proceeds as follows. The class of global patterns for each case of Theorem 4.1 is first described. The lower bound of the spatial entropy is then obtained by finding the maximal set of patching blocks of minimal size. Next, for the remaining regions of the parameter space, only finite types of global patterns appear. Therefore, it is easily seen that they are pattern formation.

Case 1. $[4, 4]_i$, $1 \le i \le 8$.

All possible local patterns are feasible and, therefore, each position can have two choices: ■ or □. Hence, the spatial entropy is ln 2.

Case 2a. $[4, 3]_{1,2}$.

Only $\begin{matrix}\blacksquare & \\ \square & \blacksquare\end{matrix}$ is infeasible. The global patterns are obtained by allowing paths of infinite length to be white and the remainders are black.

Patching blocks of size 2×2:

$$\begin{matrix}\square & \blacksquare \\ \square & \square\end{matrix}, \quad \begin{matrix}\blacksquare & \blacksquare \\ \square & \square\end{matrix}, \quad \begin{matrix}\square & \blacksquare \\ \square & \blacksquare\end{matrix}.$$

Hence, on the $2n \times 2n$ lattice, we have n^2 disjoint blocks of size 2×2 and each block have three choices. Therefore,

$$h[4, 3]_{1,2} \ge \lim_{m,n\to\infty} \frac{\ln 3^{n\cdot n}}{2n \cdot 2n} = \frac{\ln 3}{4}.$$

Case 2b. $[4, 3]_{3,4}$.

Only $\begin{matrix}\square & \\ \square & \blacksquare\end{matrix}$ is not feasible. The global patterns are obtained by allowing some nonincreasing paths U to be white, whose each downward step is at most one, i.e. if (i, j) and $(i-1, j)$ belong to U then $(i, j+1)$ must belong to U. For example,

$$\cdots \begin{matrix}\square & \square & \\ \square & \square & \\ \square & \square & \square\end{matrix}.$$

And the remainders are black.

Patching blocks of size 2×2:

$$\begin{matrix}\square & \blacksquare \\ \blacksquare & \blacksquare\end{matrix}, \quad \begin{matrix}\blacksquare & \blacksquare \\ \blacksquare & \blacksquare\end{matrix}, \quad \begin{matrix}\square & \blacksquare \\ \blacksquare & \square\end{matrix}, \quad \begin{matrix}\blacksquare & \blacksquare \\ \blacksquare & \square\end{matrix}.$$

Hence, a similar argument shows that

$$h[4, 3]_{3,4} \ge \frac{\ln 4}{4}.$$

Case 2c. $[4, 3]_{5,6}$.

In this case, only $\begin{matrix}\square & \\ \square & \square\end{matrix}$ is not feasible. The global pattern is obtained by letting some paths of $\mathbb{Z}^2$, containing no $\begin{matrix}\square & \\ \square & \square\end{matrix}$, to be white and the remainders to be black.

Patching blocks of size 2×2:

$$\begin{matrix}\square & \blacksquare \\ \blacksquare & \square\end{matrix}, \quad \begin{matrix}\square & \blacksquare \\ \blacksquare & \blacksquare\end{matrix}, \quad \begin{matrix}\blacksquare & \blacksquare \\ \blacksquare & \square\end{matrix}, \quad \begin{matrix}\blacksquare & \blacksquare \\ \blacksquare & \square\end{matrix}, \quad \begin{matrix}\square & \blacksquare \\ \blacksquare & \blacksquare\end{matrix}.$$

Spatial entropy:

$$h[4, 3]_{5,6} \ge \frac{\ln 5}{4}.$$

Case 2d. $[4, 3]_{7,8}$.

Only $\begin{matrix}\blacksquare & \\ \square & \square\end{matrix}$ is not feasible. It is the reflection of the $\begin{matrix}\square & \\ \square & \blacksquare\end{matrix}$, the only infeasible local pattern for $[4, 3]_{1,2}$, about the axis $\{(i, i) : i \in \mathbb{Z}\}$. Hence, the global patterns are obtained by reflecting those of the Case 2a with respect to the axis $\{(i, i) : i \in \mathbb{Z}\}$.

Patching blocks of size 2×2:

$$\begin{matrix}\blacksquare & \blacksquare \\ \blacksquare & \square\end{matrix}, \quad \begin{matrix}\square & \blacksquare \\ \blacksquare & \square\end{matrix}, \quad \begin{matrix}\blacksquare & \blacksquare \\ \blacksquare & \blacksquare\end{matrix}, \quad \begin{matrix}\square & \blacksquare \\ \blacksquare & \blacksquare\end{matrix}.$$

Spatial entropy:

$$h[4, 3]_{7,8} \ge \frac{\ln 4}{4}.$$

Case 3a. $[4, 2]_{4,5}$.

$\begin{matrix}\square & \\ \square & \blacksquare\end{matrix}$ and $\begin{matrix}\square & \\ \square & \square\end{matrix}$ are infeasible, i.e. more than one consecutively vertical white cells are forbidden. Hence, the global patterns are obtained by letting some horizontal edges to be white and the remainders to be black.

Patching blocks of size 2×2:

$$\begin{matrix}\square & \blacksquare \\ \blacksquare & \blacksquare\end{matrix}, \quad \begin{matrix}\square & \square \\ \blacksquare & \blacksquare\end{matrix}, \quad \begin{matrix}\blacksquare & \blacksquare \\ \blacksquare & \blacksquare\end{matrix}, \quad \begin{matrix}\blacksquare & \square \\ \blacksquare & \blacksquare\end{matrix}.$$

Spatial entropy:

$$h[4, 2]_{4,5} \ge \frac{\ln 4}{4}.$$

Case 3b. $[4, 2]_{6,7}$.

$\begin{matrix}\blacksquare & \\ \square & \square\end{matrix}$ and $\begin{matrix}\square & \\ \square & \square\end{matrix}$ are not feasible, i.e. more than one consecutively horizontal white cells are forbidden. Hence, the global patterns are obtained by allowing some vertical edges to be white and the remainders are black.

Patching blocks of size 2×2:

$$\begin{matrix}\square & \blacksquare \\ \blacksquare & \blacksquare\end{matrix}, \quad \begin{matrix}\square & \blacksquare \\ \square & \blacksquare\end{matrix}, \quad \begin{matrix}\blacksquare & \blacksquare \\ \blacksquare & \blacksquare\end{matrix}, \quad \begin{matrix}\blacksquare & \blacksquare \\ \square & \blacksquare\end{matrix}.$$

Spatial entropy:

$$h[4, 2]_{6,7} \ge \frac{\ln 4}{4}.$$

Case 4. $[4, 1]_{5,6}$.

 are not feasible. This is the union of the infeasible local patterns of Cases 2d and 3a. Hence the global patterns are the intersection of those of Cases 2d and 3a. Indeed, the global patterns are obtained by allowing some nonincreasing paths whose each downward and rightward step is at most one.

Patching blocks of size 2×2:

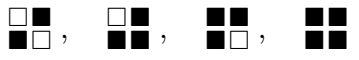

In each case $[3, 3]_i$, $1 \leq i \leq 8$, the set of feasible local patterns has the property: if a local pattern is feasible then its color-reversed pattern is also feasible. Therefore we say that the global pattern for $[\mu, \nu]_i$ has the *symmetric property* in $[\mu, \nu]_i$ if its color-reversed pattern is also for $[\mu, \nu]_i$. Obviously, every global pattern of $[3, 3]_i$ inherits the symmetric property from its feasible local patterns.

Case 5a. $[3, 3]_{1,2}$

 and  are not feasible, due to one more infeasible local pattern  than in Case 2a. The global patterns are obtained by taking those from Case 2a, which have the symmetric property in $[4, 3]_{1,2}$.

Patching block of size 4×5:

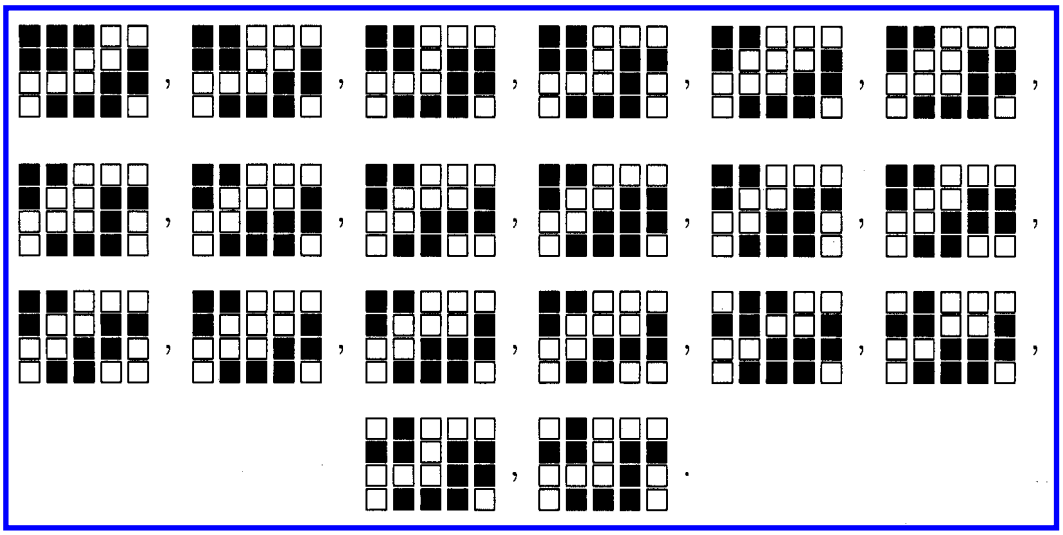

Spatial entropy:

$$h[3, 3]_{1,2} \geq \frac{\ln 20}{20}.$$

Case 5b. $[3, 3]_{3,4}$.

 and  are not feasible, due to one more infeasible local pattern  than in Case 2b. The global patterns are obtained by taking those from Case 2b, which have the symmetric property in $[4, 3]_{3,4}$.

Patching block: Patching blocks of size 3×4:

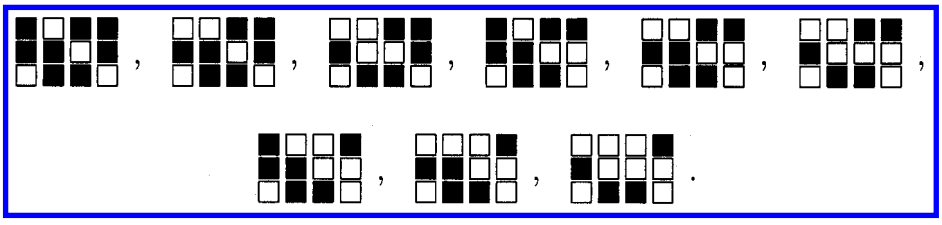

Spatial entropy:

$$h[3,\ 3]_{3,4} \geq \frac{\ln\ 9}{12}.$$

Case 5c. $[3,3]_{5,6}$.

 and  are not feasible, due to one more infeasible local pattern  than in the Case 2c. The global patterns are obtained by taking those from Case 2c, which have the symmetric property in $[4,\ 3]_{5,6}$.

Patching block of size 3×3:

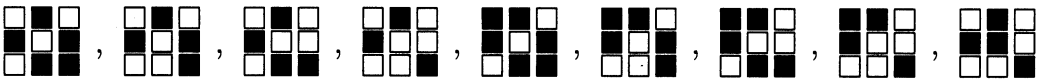

Spatial entropy:

$$h[3,\ 3]_{5,6} \geq \frac{\ln\ 9}{9}.$$

Case 5d. $[3,\ 3]_{7,8}$.

 and  are not feasible, due to one more infeasible local pattern  than in Case 2d. The global patterns are obtained by taking Case 2d those of which have the symmetric property in $[4,\ 3]_{7,8}$.

Patching blocks of size 4×3:

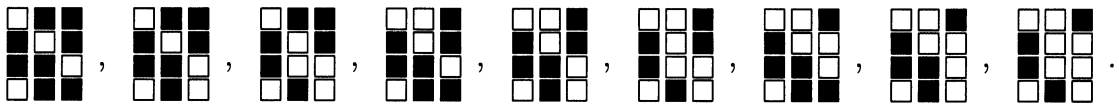

Spatial entropy:

$$h[3,\ 3]_{7,8} \geq \frac{\ln\ 9}{20}.$$

Case 6a. $[3,2]_4$.

$\left\{\right.$  ,  ,  $\left.\right\}$ are not feasible. This case has one more infeasible local pattern  than in Case 5b. Therefore, the global patterns are obtained by taking those of Case 5b, which contain no .

Patching block of size 3×4:

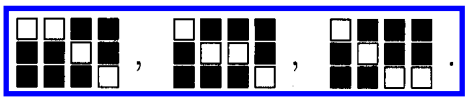

Spatial entropy:

$$h[4,\ 3]_4 \geq \frac{\ln\ 3}{12}.$$

Case 6b. $[3,\ 2]_5$.

$\left\{\right.$  ,  , $\left.\right\}$ are not feasible. This case has one more infeasible local pattern  than in Case 5c, so the global patterns are obtained by taking those from Case 5c, which contain no .

Patching blocks of size 7×3:

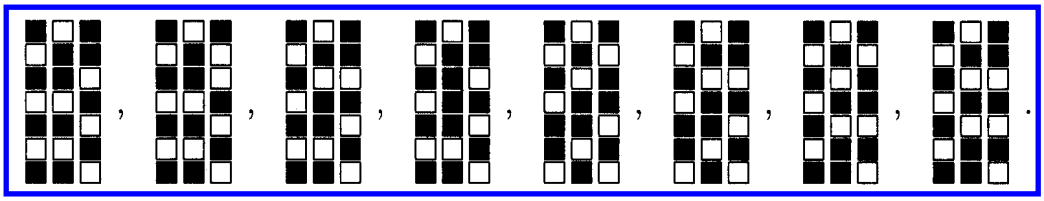

Spatial entropy:

$$h[3,\ 2]_5 \geq \frac{\ln\ 8}{21}.$$

Case 6c. $[3,\ 2]_6$.

$\left\{ \begin{smallmatrix} \blacksquare \\ \blacksquare\blacksquare \end{smallmatrix},\ \begin{smallmatrix} \square \\ \square\square \end{smallmatrix},\ \begin{smallmatrix} \blacksquare \\ \square\square \end{smallmatrix} \right\}$ are not feasible. The global patterns are obtained by reflecting those patterns for $[3,\ 2]_5$ about the axis $\{(i,\ i) : i \in \mathbb{Z}\}$.

Patching block of size 3×7:

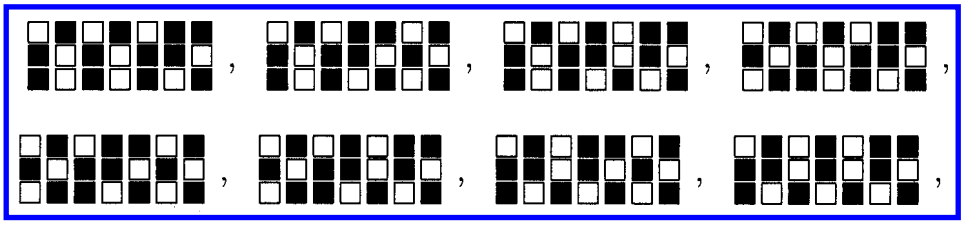

Spatial entropy:

$$h[3,\ 2]_6 \geq \frac{\ln\ 8}{21}.$$

Case 6d. $[3,\ 2]_7$.

$\left\{ \begin{smallmatrix} \square \\ \blacksquare\blacksquare \end{smallmatrix},\ \begin{smallmatrix} \blacksquare \\ \square\square \end{smallmatrix},\ \begin{smallmatrix} \square \\ \square\square \end{smallmatrix} \right\}$ are not feasible. The global patterns are obtained by reflecting those patterns for $[3,\ 2]_4$ about the axis $\{(i,\ i) : i \in \mathbb{Z}\}$.

Patching block of size 4×3:

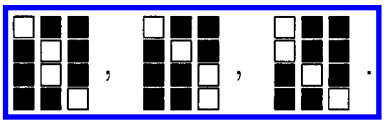

Spatial entropy:

$$h[3,\ 2]_7 \geq \frac{\ln\ 3}{15}.$$

The remaining regions of the parameter space are all pattern formation. Only finite types of patterns appear. Therefore Table 1 lists the results for each case, where $\times$ means no global patterns exist. The Appendix illustrates the type of patterns which $P_i s'$ represent.

5. Discussion

In Sec. 4, we use the maximal set of patching block of minimal size to estimate the lower bound of the spatial entropy. The reason for using the size is that it requires less time to find them. However, the set of patching blocks of a larger size will give a more precise estimate of lower bound. Indeed, denote by $B(m,\ n)$ the number of elements in the maximal set of the patching blocks of size $m \times n$. Define

$$\underline{h}_{m,n} = \frac{\ln\ B(m,\ n)}{mn},$$

the lower bound of the spatial entropy given by the maximal set of patching blocks. Proposition 5.1 indicates the superiority of the patching blocks of large size.

Table 1. The regions of pattern formation and the types of patterns appear in each region.

	R_1	R_2	R_3	R_4	R_5	R_6	R_7	R_8
[4, 2]	P1, P2 P5, P11	P1, P2, P6, P12	P1, P2, P6, P12	chaos	chaos	chaos	chaos	P1, P2, P5, P11
[4, 1]	P1, P2, P3, P4, P17	P1, P2, P3, P4, P17	P1, P8, P14	P1, P8, P14	chaos	chaos	P1, P7, P13	P1, P7, P13
[4, 0]	P1	P1	P1	P1	P1	P1	P1	P1
[3, 2]	P1, P2, P4, P5, P15, P20	P1, P2, P4, P6, P16, P21	P1, P6, P18, P22	chaos	chaos	chaos	chaos	P1, P2, P3, P19, P23
[3, 1]	P1, P2, P3, P4	P1, P2, P3, P4	P1, P8	P1, P8	P24, P25	P24, P25	P1, P7	P1, P7
[3, 0]	P1	P1	P1	P1	×	×	P1	×
[2, 2]	P1, P2, P5	P1, P2, P5	P1, P2, P6	P10, P25	P10, P25	P9, P25	P9, P25	P1, P5
[2, 1]	P1, P2, P3	P1, P2, P4	P1, P8	P25	P25	P25	P9	P1, P7
[2, 0]	P1	P1	P1	P1	×	×	×	×
[1, 1]	P1, P2	P1, P2	P10	P10	P24	P24	P9	P9
[1, 0]	P1	P1	×	×	×	×	×	×

Proposition 5.1. $\{\underline{h}_{2^k m,2^n}\}_{k=1}^{\infty}$ *is an increasing sequence.*

Proof. First, we claim that $\underline{h}_{2m,2n} \leq \underline{h}_{m,n}$ In a $2m \times 2n$ lattice, there are 2×2 disjoint blocks of size $m \times n$. When constructing the patching blocks in the lattice, each block has at least $B(m, n)$ choices i.e. $B(m, m) \leq (B(m, n))^{2\times 2}$. Hence $\overline{h}_{2m,2n} \leq \underline{h}_{m,n}$ follows immediately. The standard induction argument shows that $\{\underline{h}_{2^k m,2^k n}\}_k$ is decreasing. The proof is complete. ■

Combining the Propositions 3.1 and 5.1 we get the inequality:

$$\underline{h}_{m,n} \leq \underline{h}_{2m,2n} \leq \underline{h}_{2^2 m,2^2 n} \leq \cdots \leq \overline{h}_{2^2 m,2^2 n} \leq \overline{h}_{2m,2n} \leq \overline{h}_{m,n}.$$

References

Chow, S. N. & Mallet-Paret, J. [1995a] "Pattern formation and spatial chaos in lattice dynamical system: I," *IEEE Trans. Circuits Syst.* **42**, 746–751.

Chow, S. N. & Mallet-Paret, J. [1995b] "Pattern formation and spatial chaos in lattice dynamical system: II," *IEEE Trans. Circuits Syst.* **42**, 752–756.

Chow, S. N., Mallet-Paret, J. & Van Vleck, E. S. [1996a] "Pattern formation and spatial chaos in spatial discrete evolution equations," *Rand. Comput. Dyn.* **4**, 109–178.

Chow, S. N., Mallet-Paret, J. & Van Vleck, E. S. [1996b] "Dynamics of lattice differential equations," *Int. J. Bifurcation and Chaos* **6**(9), 1605–1622.

Chua, L. O. & Yang, L. [1988a] "Cellular neural networks: Theory," *IEEE Trans. Circuits Syst.* **35**, 1257–1272.

Chua, L. O. & Yang, L. [1988b] "Cellular neural networks: Applications," *IEEE Trans. Circuits Syst.* **35**, 1273–1290.

Chua, L. O. & Roska, T. [1990] "Stability of a class of nonreciprocal cellular neural networks," *IEEE Trans. Circuits Syst.* **40**, 1520–1527.

Chua, L. O. & Roska, T. [1993] "The CNN paradigm," *IEEE Trans. Circuits Syst.* **40**, 147–156.

Chua, L. O. [1998] *CNN: A Paradigm for Complexity*, World Scientific Series on Nonlinear Science, Series A, Vol. 31.

Crounse, K. R., Thiran, P., Setti, G. & Chua, L. O. [1997] "Characterization and dynamics of pattern formation in cellular neural networks," *Int. J. Bifurcation and Chaos* **6**(9), 1703–1724.

Hsu, C. H., Juang, J., Lin, S. S. & Lin, W. W. [2000] "Cellular neural networks: Local patterns for general template," *Int. J. Bifurcation and Chaos* **10**(7), 1645–1659

Juang, J. & Lin, S. S. [1997] "Cellular neural networks: Mosaic pattern and spatial choas," *SIAM J. Appl. Math.* **60**(3), 891–915.

Lin, S. S. & Shih, C. W. [1999] "The complete stability for standard cellular neural networks," *Int. J. Bifurcation and Chaos* **9**(5), 909–918.

Lin, S. S. & Yang, T. S. [2000] "Spatial entropy of 1-dimensional cellular neural networks," *Int. J. Bifurcation and Chaos* **10**(9), 2129–2140.

Robinson, C. [1995] *Dynamical Systems: Stability, Symbolic Dynamics, and Chaos* (CRC Press, Boca Raton, FL).

Setti, G., Thiran, P. & Serpico, C. [1998] "An approach to information propagation in 1-D cellular neural networks — Part II: Global propagation," *IEEE Trans. Circuits Syst.* **45**, 790–811.

Shih, C. W. [1998] "Pattern formation and spatial chaos for cellular neural networks with asymmetric templates," *Int. J. Bifurcation and Chaos* **8**(10), 1907–1936.

Thiran, P., Crounse, K. R., Chua, L. O. & Hasler, M. [1995] "Pattern formation properties of autonomous cellular neural networks," *IEEE Trans. Circuits Syst.* **42**, 757–774.

Thiran, P., Setti, G. & Hasler, M. [1998] "An approach to information propagation in 1-D cellular neural networks — Part I: Local diffusion," *IEEE Trans. Circuits Syst.* **45**, 777–789.

Appendix

P1: pattern of all black.

P2: pattern of all white.

P3: $\mathbb{Z}^2$ is divided into two parts — all black and all white. The boundary of the two parts is a vertical line.

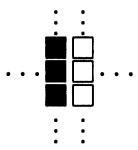

P4: $\mathbb{Z}^2$ is divided into two parts — all black and all white. The boundary of the two parts is a horizontal line.

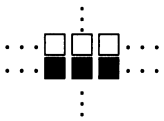

P5: Each vertical line is either all black or all white.

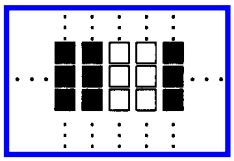

P6: Each horizontal line is either all black or all white.

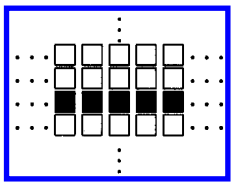

P7: Each vertical line is either all black or all white and the vertical white line is adjacent to only black lines.

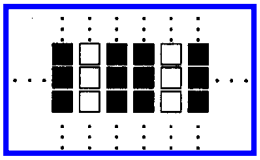

P8: Each horizontal line is either all black or all white and the horizontal white line is adjacent to only black lines.

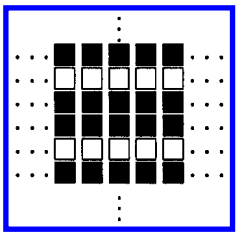

P9: Each vertical line is either all black or all white and every two adjacent vertical lines have different colors.

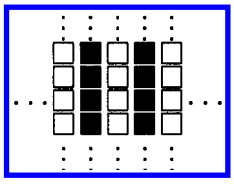

P10: Each horizontal line is either all black or all white and every two adjacent horizontal lines have

different colors.

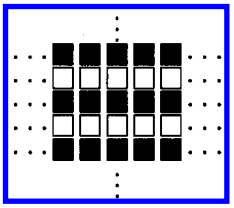

P11: The vertical lines are of only two types: (a) whole black or white and (b) upper half white and lower half black.

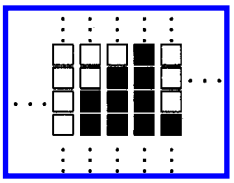

P12: The horizontal lines are of only two types: (a) whole black or white and (b) left half black and right half white.

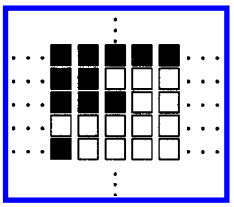

P13: The vertical lines are of two types: (a) all black or white. (b) upper half white and lower half black. And (b) is adjacent to vertical black lines.

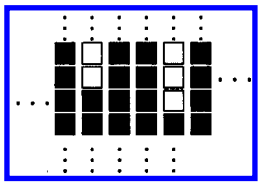

P14: The horizontal lines are of two types: (a) all black or white. (b) upper half black and lower half black. And (b) is adjacent to the horizontal white lines.

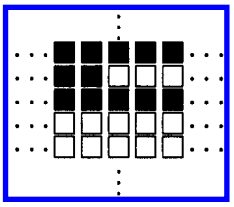

P15: $\mathbb{Z}^2$ is divided into two parts: the left part is entirely white and the right part is entirely black. The boundary of the two parts is a nondecreasing path.

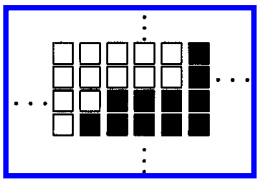

P16: $\mathbb{Z}^2$ is divided into two parts: the left part is all black and the right part is all white. The boundary of the two parts is a nondecreasing path.

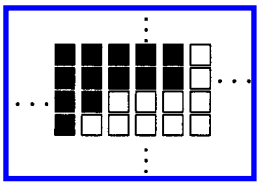

P17: $\mathbb{Z}^2$ is divided into two parts. The left part is all black and the right part is all white. The boundary of the two parts is a nonincreasing path.

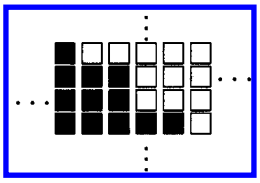

P18: $\mathbb{Z}^2$ is divided into two parts. The left part is all white and the right part is all black. The boundary of the two parts is a strictly decreasing path whose each downward step is at most one.

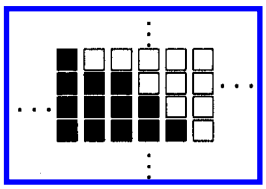

P19: $\mathbb{Z}^2$ is divided into two parts. The left part is all white and the right part is all black. The boundary of the two parts is a strictly decreasing path whose each rightward step is at most one.

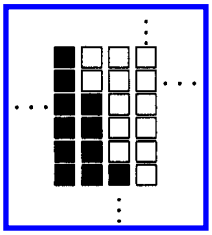

P20: This is a mixed type of P15 and P5. Indeed, the pattern consists of (a) P15 with finite width and (b) vertical lines of all black or all white. And (a) is

adjacent to a vertical white line on the right and a white or black vertical line on the left, respectively.

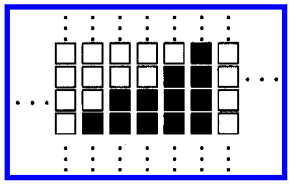

P21: This is a mixed type of P16 and P6. Indeed, the pattern consists of (a) P16 with finite height and (b) horizontal lines of all black or all white. And (a) is adjacent above to a horizontal black line and below a horizontal white line, respectively.

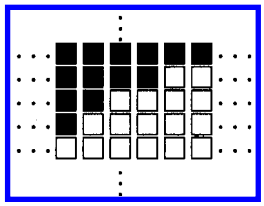

P22: This is a mixed type of P17 and P6. Indeed, the pattern consists of (a) P17 with finite height and (b) horizontal lines of all black or all white. And (a) is adjacent above to a horizontal white line and below a white or black horizontal line, respectively.

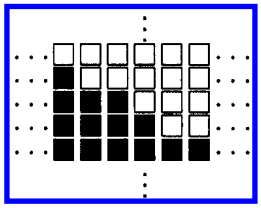

P23: This is a mixed type of P18 and P5. Indeed, the pattern consists of (a) P18 with finite width and (b) vertical lines of all black or all white. And (a) is adjacent to vertical lines.

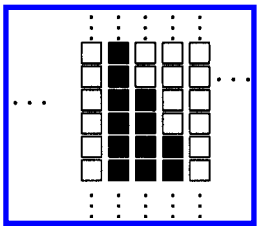

P24: Checkerboard.

P25: